

HiMix: Reducing Computational Complexity in Large Vision-Language Models

Xuange Zhang^{1†}, Dengjie Li^{2†}, Bo Liu¹, Zenghao Bao², Yao Zhou², Baisong Yang², Zhongying Liu²,
Yujie Zhong², Zheng Zhao^{2*}, Tongtong Yuan^{1*}

¹Beijing University of Technology, CN ²Meituan Inc., CN

szxg923@emails.bjut.edu.cn, {liubo, yuantt}@bjut.edu.cn,

{lidengjie, baozenghao, zhouyao11, yangbaisong02, liuzhongying, zhongyujie, zhaozheng08}@meituan.com

Abstract

Benefiting from recent advancements in large language models and modality alignment techniques, existing Large Vision-Language Models (LVLMs) have achieved prominent performance across a wide range of scenarios. However, the excessive computational complexity limits the widespread use of these models in practical applications. We argue that one main bottleneck in computational complexity is caused by the involvement of redundant vision sequences in model computation. This is inspired by a re-assessment of the efficiency of vision and language information transmission in the language decoder of LVLMs. Then, we propose a novel hierarchical vision-language interaction mechanism called Hierarchical Vision injection for Mixture Attention (HiMix). In HiMix, only the language sequence undergoes full forward propagation, while the vision sequence interacts with the language at specific stages within each language decoder layer. It is striking that our approach significantly reduces computational complexity with minimal performance loss. Specifically, HiMix achieves a 10× reduction in the computational cost of the language decoder across multiple LVLM models while maintaining comparable performance. This highlights the advantages of our method, and we hope our research brings new perspectives to the field of vision-language understanding. Project Page: <https://xuange923.github.io/HiMix/>

1. Introduction

”What I hear, I forget. What I see, I remember.”

—— Confucius

Understanding complex content is a pivotal step toward artificial general intelligence (AGI). As the two core modalities of information processing, vision and language each

[†]Equal Contribution. ^{*}Corresponding author. Work was done when Xuange Zhang was an intern at Meituan Inc.

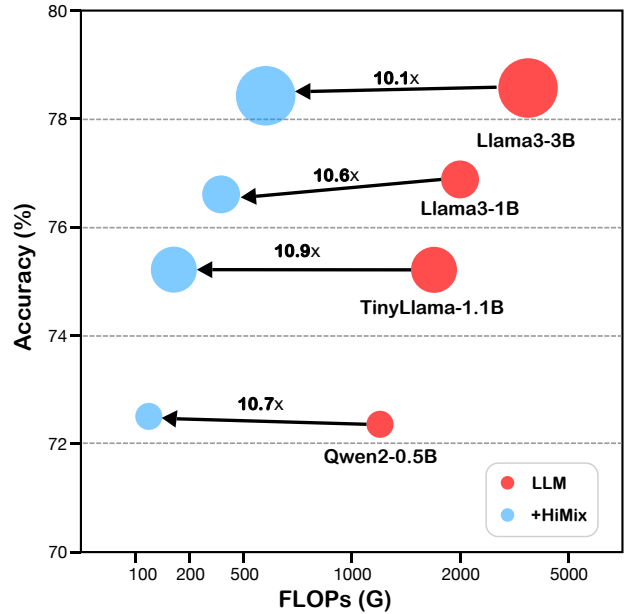


Figure 1. Comparison of performance and computational cost of the language decoder between the original and HiMix models. The circles, arranged from smallest to largest, represent the models Qwen2-0.5B, Llama3-1B, TinyLlama-1.1B, and Llama3-3B. While maintaining a similar performance to the original models, our HiMix achieves a 10× reduction in computational cost.

have unique advantages: *text* can provide detailed semantic information, while *image* can present intuitive vision cues. How to effectively integrate information from these two modalities has become a crucial orientation of current research. We have witnessed tremendous research and effort to achieve more complex and higher levels of semantic understanding built upon multimodal information integration [3, 13, 16, 20, 21, 25, 39]. Most models integrate vision and language features by concatenating them for input into Large Language Model (LLM) [1, 12, 14]. However, vision sequences are typically longer than language sequences, significantly increasing computational complex-

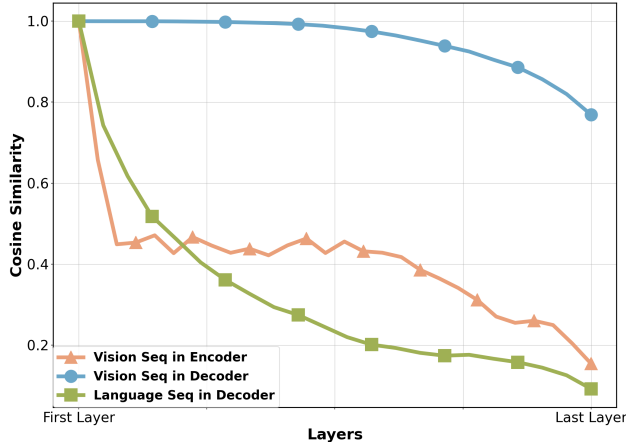


Figure 2. Layer-wise Cosine Similarity of Vision and Language Sequences.

ity. This prompts us to wonder: *Is simple concatenation truly the most efficient approach for facilitating interaction between vision and language?*

Inspired by the famous quote of *Confucius*, we begin to consider the role of visual and language information in the language decoder of LVLMs. We hypothesize that, during the forward propagation process, vision information may not need to be involved throughout the entire process. A classic example is the story about the Treasure Hunt: the protagonist in the story typically has text information in the form of a *riddle* and image information in the form of a *map*. During the treasure hunt, the protagonist usually focuses on understanding the instructions in the riddle, consulting the map only when necessary to determine the direction. This analogy suggests that, as the backbone of the LVLM, the language model should primarily focus on *text* for comprehension and processing tasks, referring to *image* only when additional support is required.

Therefore, we further analyze the layer-wise divergences generated during the forward propagation of vision and language sequences to support this hypothesis. Specifically, we examine the divergences between the original sequences input to the language decoder and the vision encoder of the LVLM, and the output sequences of each layer. The divergences are measured by cosine similarity, as shown in Figure 2. It is obvious that in the vision encoder, the divergence of vision sequences shows significant changes from shallow to deep layers. This implies that as the model deepens, the vision encoder can capture higher-level semantic information. However, in the language decoder, the divergence between the vision sequences and the original sequences is much smaller compared to the language sequences. This reveals that vision sequences are updated less during forward propagation and are not the primary focus of the model, which undoubtedly supports our hypothesis. We boldly

speculate that it is feasible to remove vision sequences from the forward propagation in the language decoder of the LVLM. By incorporating these sequences only at specific stages, we can achieve comparable performance while significantly reducing overall computational complexity.

Based on these insights, we introduce **Hierarchical Vision injection for Mixture Attention (HiMix)**, a novel vision-language interaction mechanism for MLLMs. Our method avoids concatenating vision and language sequences as input. Instead, only the language sequence is involved in the entire forward propagation, while the vision sequence is injected at specific stages within each layer to interact with the language through Mixture Attention. This approach allows the model to receive more diverse vision inputs while significantly reducing overall computational complexity. As shown in Figure 1, HiMix reduces the computational cost to approximately $10\times$ lower than that of the original model across various base models, while maintaining comparable performance, highlighting the significant advantage of our method in boosting computational efficiency. The main contributions of our work are as follows:

- We hypothesize that visual information is not necessary throughout the forward propagation process in the language decoder of the LVLM.
- We introduce a novel vision-language interaction mechanism in which only the language sequence undergoes full forward propagation, while vision sequences are injected at specific stages to enhance the model’s performance.
- Our HiMix maintains competitive performance on various models, *e.g.*, Qwen2 and Llama3, while achieving $10\times$ reductions on computational complexity.

2. Related Works

2.1. Large Vision-Language Models

With the remarkable performance of LLMs [1, 4, 28, 29, 35, 37] in natural language processing, researchers have extended these models to the multimodal domain, enabling more advanced vision and language understanding tasks. The typical architecture of LVLMs [5, 11, 25, 38, 39] includes three main components: a visual encoder, a vision-language connector, and a large language model. Most approaches focus on aligning visual features with the textual space effectively. In this field, Flamingo [2] pioneers the use of resamplers and cross-attention dense blocks to integrate visual features into LLMs. Following this, BLIP-2 [21] introduces Qformer, which leverages frozen image encoders and LLMs to perform various vision-language tasks. The LLaVA series [19, 24, 25] and MiniGPT-4 [39] apply simple but effective projection layers to align different modalities and improved instruction-following abilities through multimodal instruction tuning data. Fuyu [6] aligns image patches to the LLM embeddings through a simple lin-

ear mapping. InternVL [11] introduces a large-scale vision encoder that integrates with QLLaMA as middleware for alignment with the LLM. Qwen-VL [5] proposes a Position-aware Vision-Language Adapter, which compresses visual feature sequences to a fixed length before input to the LLM.

However, as model sizes continue to increase, the computational resources required also grow, calling for more efficient input processing methods to manage the increasing contextual demands.

2.2. Vision Token Reduction

The primary reason for the high computational cost of LVLMs is the excessive length of input sequences, often due to numerous prefix visual tokens. As computational costs scale quadratically with the number of input tokens, researchers have explored methods to reduce visual tokens and thereby lower computational expenses effectively.

FastV [10] is among the first to identify the inefficiencies associated with visual token usage in LVLMs. This model uses signals from the LLM to guide visual token pruning, trimming half of the image tokens within intermediate layers of the LLM. VTW [23] takes this further by completely removing all visual tokens after a certain intermediate layer, relying only on text tokens for subsequent computations. LLaVA-PruMerge [26] dynamically retains visual tokens based on their similarity, effectively compressing the number of visual tokens. M^3 [7], inspired by Matryoshka Representation Learning, learns multi-granular, coarse-to-fine token representations to control the number of tokens involved in computation.

While these approaches effectively reduce computational loads, they primarily focus on pruning or fully excluding visual tokens from certain computations. In contrast, our HiMix method avoids involving vision sequences in the forward propagation process. Rather than merely trimming or excluding visual tokens, HiMix hierarchically injects vision information at specific stages, allowing the model to reference visual cues only when necessary. This approach significantly reduces computational cost while preserving model performance.

3. Method

This paper presents a novel approach to vision-language understanding by modifying the interaction between multimodal information. In the preliminary section, we briefly introduce the commonly used LVLM method, referred to as the Vanilla-LVLM, followed by a detailed description of our proposed HiMix structure.

3.1. Preliminary

For an input image I , we extract the vision feature sequence $X_v = f_{VE}(I)$ using a pre-trained vision encoder. In the Vanilla-LVLM, these vision features are transformed

through a connector to align with the language features, producing a sequence $X_{v'} \in \mathbb{R}^{N \times d}$, where N is the length of the vision sequence and d is the feature dimension. For the input text T , features are extracted using a text encoder bonded to the LLM: $X_l = f_{TE}(T)$, where $X_l \in \mathbb{R}^{M \times d}$ denotes the language feature sequence, with M as the length of the language sequence.

In the Vanilla-LVLM, the concatenation of the vision and language sequences is fed into the LLM:

$$X_{vl} = [X_{v'}; X_l] \quad (1)$$

Each Transformer layer comprises two sub-layers: a self-attention layer and a feed-forward network (FFN). The attention layer includes three linear transformation matrices, W^Q , W^K , and W^V , which transform the input X_{vl} into Q , K , and V matrices. Subsequently, self-attention enables interaction within the sequence:

$$\text{SA} = \text{Softmax} \left(\frac{QK^T}{\sqrt{d}} \right) V \quad (2)$$

A causal mask is used during attention to prevent information leakage from future tokens. Following self-attention, the FFN typically consists of two linear transformation layers with a nonlinear activation function. The output A of the self-attention layer is fed into the FFN as input:

$$\text{FFN} = W_2(\text{Act}(W_1 A)) \quad (3)$$

where W_1 and W_2 are the weight matrices for linear transformations. The overall architecture of the Vanilla-LVLM is shown on the left side of Figure 3.

For an input sequence of length $N + M$, the computational complexity of the Vanilla Model includes two parts: self-attention requires $O((N + M)^2 d)$ due to the QK^T operation, while the feed-forward network, with two linear layers, contributes $O(8(N + M)d^2)$. Thus, the total complexity is:

$$O((N + M)^2 d) + O(8(N + M)d^2) \quad (4)$$

Since the vision sequence length N is usually longer than the language sequence length M , reducing the number of vision tokens in computation can effectively decrease overall computational costs.

3.2. HiMix

We introduce **H**ierarchical Vision injection for **M**ixture Attention (HiMix), designed to reduce computational complexity while maintaining LVLM performance. The key is that the vision sequence does not need to participate in the entire forward propagation process. In this section, we describe the design of Hierarchical Vision Injection and the implementation of Mixture Attention. The middle part of Figure 3 illustrates the overall structure of HiMix, while the right side shows the detailed implementation of Mixture Attention.

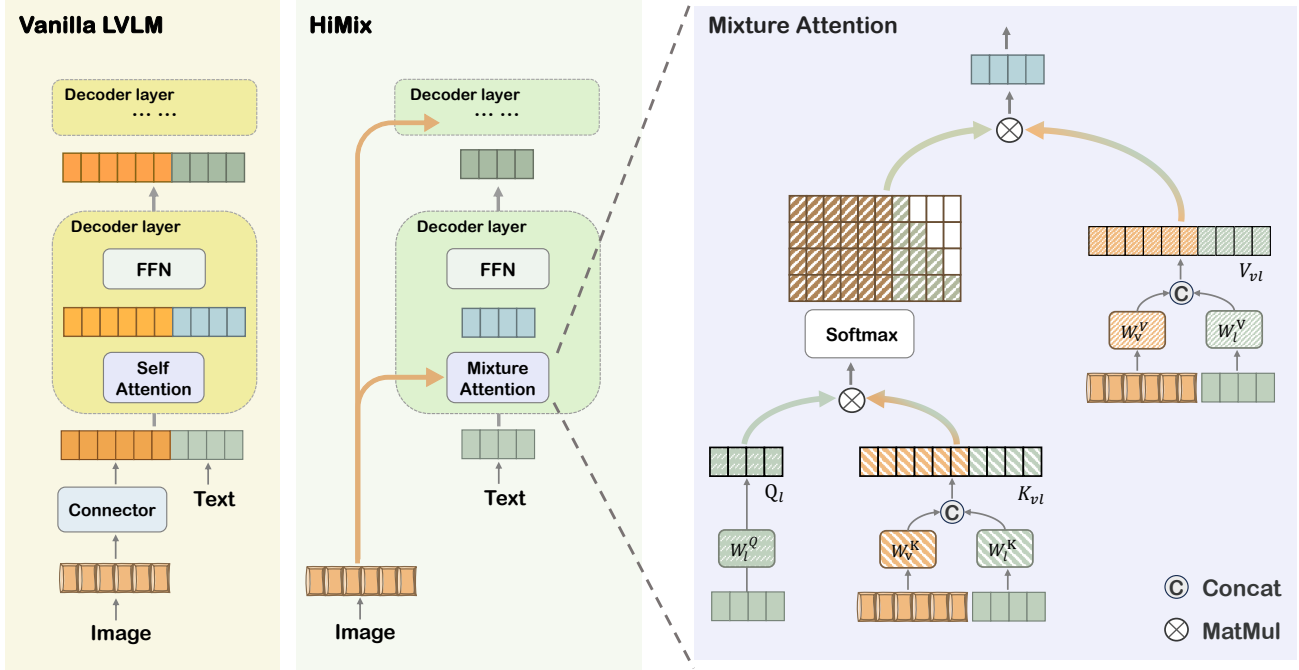


Figure 3. Comparison of Vanilla Model and HiMix Architectures. **Left:** Overall structure of traditional Vanilla. **Middle:** Overall structure of HiMix. **Right:** Details of HiMix.

3.2.1. Hierarchical Vision Injection

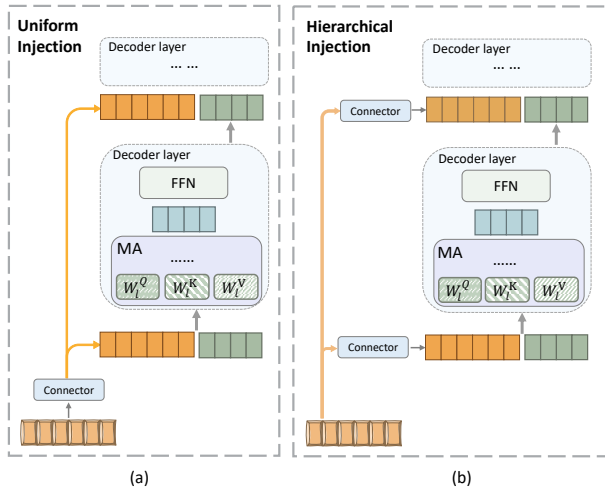


Figure 4. Exploration of Model Architecture Design. (a) Uniform Vision Injection to Each Layer. (b) Hierarchical Vision Injection Through Multi-Level Connectors. The Mixture Attention (MA) differs from the main method in that the vision and language sequences share the KV projection layers

We assume the vision sequence only needs to be injected when necessary, without being passed in layers.

A straightforward approach is to directly feed X_v into

every layer, as shown in Figure 4 (a), which represents uniform vision injection. However, this may constrain the model’s ability to effectively capture diverse vision information.

To provide the model with more diverse vision cues, an improved strategy is to increase the number of connectors to match the LLM layers, as illustrated in Figure 4 (b). The vision sequence X_v is first transformed by a corresponding connector before being fed into each layer, achieving hierarchical vision injection.

However, these structures have a common issue: in subsequent attention computations, the vision and language sequences share the same KV projection layers. This may not be the most optimal solution. Since the language sequence undergoes attention and passes through the feed-forward network (FFN) at each layer, sharing the same KV projections with the vision sequence could introduce interference between the two modalities.

In our final model, we address this issue by merging each connector with the projection layers, resulting in dedicated vision projection layers. These layers not only align the dimensions between the modalities but also enable the hierarchical injection of vision features in the most straightforward manner. Finally, we send the vision sequence X_v to each layer and integrate the vision projection layers into the attention mechanism, ensuring no interference between the vision and language sequences.

3.2.2. Mixture Attention

In Mixture Attention, the vision sequence X_v and language sequence X_l are treated as two separate inputs.

Initially, the inputs are processed through five linear transformation matrices. Vision features are transformed through W_v^K and W_v^V to produce matrices K_v and V_v . Language features are transformed via W_l^Q , W_l^K , W_l^V to produce matrices Q_l , K_l , and V_l .

We then concatenate the vision and language information to form the complete **KV** sequence:

$$K_{vl} = [K_v; K_l], \quad V_{vl} = [V_v; V_l] \quad (5)$$

Subsequently, mixture attention facilitates multimodal information interaction:

$$\text{MA} = \text{Softmax} \left(\frac{Q_l K_{vl}^T}{\sqrt{d}} \right) V_{vl} \quad (6)$$

The resulting sequence maintains the same length as the initial language feature sequence, and the vision sequence does not require forward propagation.

During the attention calculation, positional embeddings are added to Q_l and K_l . Note that since the vision features already contain positional information from feature extraction, we do not add additional positional embedding to the vision sequence.

We apply a part-causal mask to the attention weights: all language tokens can attend to previous vision tokens, while a causal mask is applied for language interactions to prevent future information leakage.

For an input sequence of length $N + M$, the computational complexity of HiMix includes two parts: mixture attention requires $O((N + M)Md)$ due to the $Q_l K_{vl}^T$ operation, while the feed-forward network, applied only to the language sequence, contributes $O(8Md^2)$. Thus, the total complexity is:

$$O((N + M)Md) + O(8Md^2) \quad (7)$$

Compared to the complexity of the Vanilla-LVLM, HiMix significantly reduces computational cost. By avoiding the quadratic term associated with self-attention across both sequences, HiMix provides a more efficient solution, especially advantageous for handling longer vision sequences.

The complete algorithmic workflow of HiMix is presented in Algorithm 1.

4. Experiments

In this section, we first introduce the experimental setup, followed by a detailed discussion of the ablation study, analyzing the impact of each component on model performance and efficiency. Next, we present the main experimental results, demonstrating the effectiveness of the proposed HiMix method across multiple benchmarks. Finally, we conduct additional extended experiments.

Algorithm 1 HiMix: Hierarchical Vision Injection for Mixture Attention

```

1: Input: Image  $I$ , Text  $T$ 
2: Output: Language sequence  $Y_l$  after  $l$  layers of processing
3: Initialize:
4:    $X_v \leftarrow f_{\text{VE}}(I)$ 
5:    $X_l \leftarrow f_{\text{TE}}(T)$ 
6:    $Y_0 \leftarrow X_l$ 
7: for  $i = 1$  to  $l$  do
8:   Language Projection:
9:      $Q_l^i, K_l^i, V_l^i \leftarrow \text{Proj}_l(Y_{i-1})$ 
10:  Vision Projection:
11:     $K_v^i, V_v^i \leftarrow \text{Proj}_v(X_v)$ 
12:  Add Positional Embedding:
13:     $Q_l^i \leftarrow Q_l^i + P_l, K_l^i \leftarrow K_l^i + P_l$ 
14:  Concatenate Sequences:
15:     $K_{vl}^i \leftarrow [K_v^i; K_l^i], V_{vl}^i \leftarrow [V_v^i; V_l^i]$ 
16:  Calculate Attention Scores:
17:     $S^i \leftarrow (Q_l^i (K_{vl}^i)^T) / \sqrt{d}$ 
18:  Apply Part-Causal Mask:
19:     $\hat{S}^i \leftarrow S^i + \text{Mask}$ 
20:  Compute Attention Output:
21:     $A_i \leftarrow \text{Softmax}(\hat{S}^i) V_{vl}^i$ 
22:  Feed-forward Network:
23:     $Y_i \leftarrow W_2(\text{Act}(W_1 A_i))$ 
24: end for
25: return  $Y_l$ 

```

4.1. Experimental Setup

Model Selection. We select TinyLlama [37], Qwen2 [32], and Llama3.2 [14] as language decoders, with the pre-trained Siglip [36] vision encoder SoViT-400m/14 as the vision encoder. In the vanilla-LVLM setup, a 2-layer MLP serves as the connector between the vision encoder and language decoder, similar to the configuration in TinyLLaVA [38]. During initialization, the corresponding pre-trained weights are loaded, and the parameters of the vision projection layers are randomly initialized.

Evaluation Metrics. To evaluate our proposed HiMix method, we assess both model efficiency and performance metrics. The experiments are designed to validate whether HiMix could significantly reduce computational complexity while maintaining competitive performance.

For model efficiency, we report the number of model parameters and computational costs (in GFLOPs). Each input sample contains an image with 728 vision tokens processed by the Siglip encoder and a text prompt sequence of length 64. This setup simulates a typical multimodal input scenario found in real-world applications.

For model performance, we evaluate the model on seven commonly used benchmarks: VQAv2 [17], GQA [18],

TextVQA [27], MM-Vet [33], POPE [22], MME [15], and MMMU [34]. These benchmarks comprehensively measure model capabilities, ranging from basic vision perception to advanced reasoning.

Training Strategies. We adopt two distinct training strategies, referred to as "Regular Paradigm" and "Enhanced Paradigm":

- *Regular Paradigm.* This strategy uses the LLaVA-1.5 [25] dataset for training. The model is first pretrained with LLaVA-1.5-558k, where the vision encoder and language decoder parameters are kept frozen, and only the vision projection layers are trained. In the supervised fine-tuning (SFT) stage, the model is fine-tuned with LLaVA-1.5-mix-665k, keeping the vision encoder frozen but updating all parameters of the language decoder.
- *Enhanced Paradigm.* This strategy leverages both the LLaVA-1.5 [25] and ShareGPT4V [8] datasets to further enhance performance, following a three-stage training approach inspired by TinyLLaVA [38]. The initial pre-training stage mirrors the setup in the Regular Paradigm. Next, the model undergoes additional pretraining with the ShareGPT4V-pretrain-1246k dataset, followed by fine-tuning with the ShareGPT4V-mix-665k dataset in the SFT stage. Both the additional pretraining and SFT stages use the same configuration as the SFT stage in the Regular Paradigm.

For the main experiments, both training strategies are applied, while the ablation studies use the Regular Paradigm."

4.2. Ablation Study

Self-Attention vs Mixture Attention. We first examine the impact on model efficiency when Self-Attention in the language decoder is replaced with Mixture Attention, the overall structure illustrated in Figure 4(a). Siglip is used as the vision encoder, and Llama3-1B is used as the language decoder. As shown in Table 1, without increasing parameter count, Mixture Attention significantly reduces computational overhead. The overall computational cost (GFLOPs) of HiMix is only 33% of that of the original model, while the computational cost of the language decoder alone is reduced to approximately 10% of the original. These results demonstrate that Mixture Attention enables efficient multimodal information interaction, greatly reducing computational costs.

Table 1. Efficiency Comparison between Models with Self-Attention and Mixture Attention. S represents Siglip. L represents Llama3-1B.

Method	Overall		Language Decoder		Vision Encoder	
	Params (B)	FLOPs (G)	Params (B)	FLOPs (G)	Params (B)	FLOPs (G)
S+L	1.67	2720	1.24	2040	0.43	671
w.MA	1.67	894(33%)	1.24	214(10%)	0.43	671

Uniform Injection vs Hierarchical Injection. We next investigate the impact of different vision injection strategies on model performance by comparing uniform vision injection with hierarchical injection. As presented in Table 2, uniform injection of vision information across all layers (illustrated in Figure 4(a)) leads to a decline in model performance, while hierarchical injection (illustrated in Figure 4(b)) improves overall performance. Although hierarchical injection incurs slightly higher computational cost compared to uniform injection, it still reduces the overall computational cost by nearly 10x compared to the original approach. Given that hierarchical injection provides more diverse vision information, it enables the model to better handle more complex tasks. This demonstrates that a hierarchical structure is a more effective approach, striking a better balance between performance and computational efficiency.

Table 2. Performance Comparison Between Uniform and Hierarchical Vision Injection.

Decoder	VQA ^{v2}	GQA	VQA ^T	POPE	MME	FLOPs(G)
Llama3-1B	76.8	59.6	52.7	86.7	1335.0	2030
w.Uniform	74.9	57.8	49.7	85.8	1243.9	201
w.Hierarchical	77.3	60.7	50.4	85.9	1260.4	354

4.3. Comprehensive Assessment

We apply HiMix across several popular language decoders to assess its generalizability, with Siglip as the vision encoder in all experiments.

Regular Paradigm Results. The results, as shown in Table 3, indicate that HiMix maintains comparable performance to the baseline model on most benchmarks, while significantly reducing computational cost. This demonstrates that our method achieves a successful balance between efficiency and effectiveness. We noticed a decline in model performance on TextVQA and MME tasks, primarily due to a decrease in OCR capability.

Enhanced Paradigm Results. To achieve better performance, we evaluated HiMix using the Enhanced Paradigm strategy. Table 4 shows that adding additional training data improves performance. Figure 5 illustrates performance gaps between the HiMix and the baseline model under two training strategies, demonstrating that Enhanced Paradigm amplifies advantage of HiMix, generally outperforms the baseline in this setup.

Efficiency Analysis. We conduct a comprehensive analysis of the computational efficiency of HiMix compared to baseline LLM models. The evaluation includes the computational cost (GFLOPs) of the language decoder and the maximum VRAM usage across varying ratios of vision-to-language input lengths. As shown in Table 5, models using HiMix demonstrate substantial reductions in computational

Table 3. Comprehensive comparison of performance and computational efficiency between the original model and HiMix **under the Regular Paradigm**, using SigLIP as the vision encoder. Performance metrics include VQAv2, GQA, TextVQA, MM-Vet, POPE, MME, and MMMU. Computational efficiency is assessed by Language Decoder parameter count (B) and GFLOPs. Performance improvements are highlighted in **bold**, with computational cost shown in **red** as a percentage of the original model.

Language Decoder	Performances							Efficiency	
	VQAv ² [17]	GQA [18]	VQA ^T [27]	MM-Vet [33]	POPE [22]	MME [15]	MMMU [34]	Params (B)	FLOPs (G)
Qwen2-0.5B	72.3	55.8	45.2	19.5	86.6	1153.0	29.7	0.49	837
+HiMix	72.6	55.9	44.2	21.1	84.9	1039.7	31.6	0.50	78(9%)
TinyLlama-1.1B	75.5	58.6	49.6	23.5	86.3	1256.5	28.3	1.10	1750
+HiMix	75.5	59.2	44.1	24.5	85.7	1179.0	29.0	1.11	161(9%)
Llama-3.2-1B	76.8	59.6	52.7	27.8	86.7	1334.5	30.6	1.24	2040
+HiMix	76.2	59.6	50.5	28.4	86.6	1198.6	29.9	1.25	192(9%)
Llama-3.2-3B	78.6	62.5	55.3	31.5	86.9	1449.3	34.8	3.21	5310
+HiMix	78.4	61.4	54.4	30.2	86.6	1261.9	35.6	3.28	525(9%)

Table 4. Comprehensive comparison of performance and computational efficiency between the original model and HiMix **under the Enhanced Paradigm**, using SigLIP as the vision encoder. Performance improvements are highlighted in **bold**, with computational cost shown in **red** as a percentage of the original model.

Language Decoder	Performances							Efficiency	
	VQAv ² [17]	GQA [18]	VQA ^T [27]	MM-Vet [33]	POPE [22]	MME [15]	MMMU [34]	Params (B)	FLOPs (G)
Qwen2-0.5B	75.6	58.7	49.0	23.1	86.9	1255.6	31.2	0.49	837
+HiMix	78.2	61.5	46.1	26.7	87.5	1162.1	29.7	0.50	78(9%)
TinyLlama-1.1B	76.7	59.8	51.8	24.7	85.8	1271.6	29.1	1.10	1750
+HiMix	78.7	61.9	50.0	26.4	86.5	1261.7	29.3	1.11	161(9%)
Llama-3.2-1B	78.2	60.9	53.8	29.2	86.6	1341.5	30.1	1.24	2040
+HiMix	79.1	61.3	51.9	29.9	86.8	1271.7	29.9	1.25	192(9%)
Llama-3.2-3B	80.2	63.4	59.5	35.4	86.6	1452.6	36	3.21	5310
+HiMix	80.2	61.7	55.2	31.7	86.8	1343.8	31.7	3.28	525(9%)

Table 5. Efficiency Comparison of Baseline and HiMix across Different Input Scenarios. V:L represents the ratio of vision to language token lengths in the input sequence. FLOPs indicates the computational cost of the language decoder, and Max VRAM refers to the maximum GPU memory required during computation.

Method	V:L 728:32		V:L 728:64		V:L 728:200		V:L 728:728		V:L 728:1000	
	FLOPs (G)	Max VRAM(GB)	FLOPs (G)	Max VRAM(GB)	FLOPs (G)	Max VRAM(GB)	FLOPs (G)	Max VRAM(GB)	FLOPs (G)	Max VRAM(GB)
Qwen2-0.5B	801	7.41	837	7.56	991	8.32	1620	11.95	1970	14.22
+HiMix	44	4.82	78	4.95	224	5.52	821	8.47	1150	10.34
TinyLlama-1.1B	1680	9.15	1750	9.35	2080	10.65	3400	16.95	4120	21.04
+HiMix	92	5.29	161	5.46	466	6.35	1720	11.12	2400	14.42
Llama-3.2-1B	1950	8.84	2040	9.05	2410	10.1	3880	15.17	4660	18.35
+HiMix	110	5.44	192	5.6	546	6.38	1970	10.32	2730	12.96
Llama-3.2-3B	5080	14.89	5310	15.24	6260	16.83	10090	24.28	12130	28.92
+HiMix	310	9.58	525	9.84	1450	11.1	5140	17.02	7120	20.9

costs and memory usage. Specifically, scenarios with V:L of 728:32 and 728:64 closely resemble typical multimodal input configurations. HiMix achieves a significant reduction in computational cost when language sequences are much shorter than vision sequences. Even as the length of the language sequence increases, HiMix consistently exhibits lower computational costs and VRAM consumption. When the input vision and language sequence lengths are equal, HiMix consumes only half the computational cost of base-

line models. This suggests that HiMix is well-suited for both general applications and more complex language processing tasks, providing substantial efficiency advantages over traditional methods.

4.4. Extended Evaluation

By adopting HiMix, the computational cost of the language decoder significantly decreases, with the vision encoder accounts for the majority of the overall computational cost.

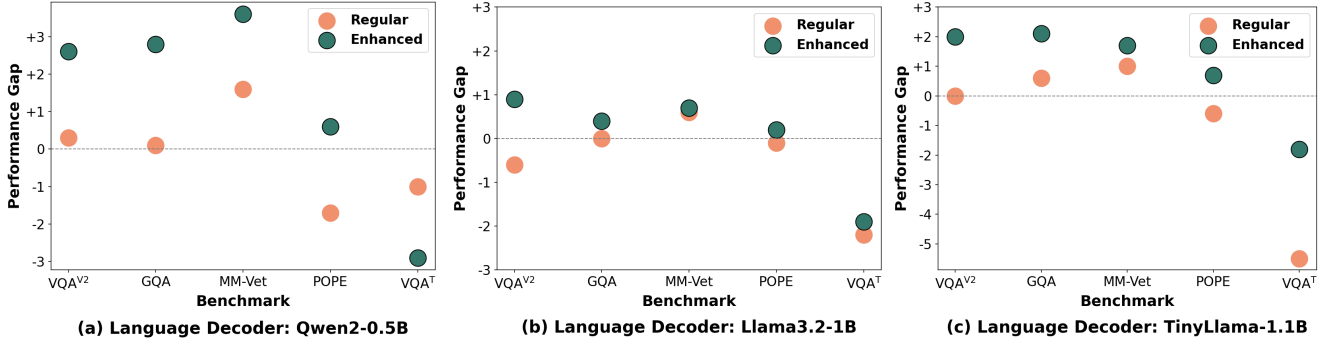


Figure 5. Performance gaps between HiMix and the baseline model across various benchmarks under two training strategies: **Regular Paradigm** and **Enhanced Paradigm**. The y-axis represents the performance gap relative to the baseline, with positive values indicating improvements. Subfigures (a), (b), and (c) show results for Qwen2-0.5B, Llama3-1B, and TinyLLaMA-1.1B, respectively. Results indicate that using the Enhanced Paradigm amplifies HiMix’s performance benefits over the baseline.

Table 6. Performance and Parameters of Various Vision Encoders. All experiments use TinyLlama-1.1B (with HiMix applied) as the language decoder. InRes: Input Image Resolution; PatchSz: Patch Size; FeatDim: Vision Feature Dimensions (Token Count, Feature Dimension).

Vision Encoder	Model Parameters					Performances				
	InRes (H×W)	PatchSz (H×W)	FeatDim	Params (B)	FLOPs (G)	VQA ^{v2}	GQA	VQA ^T	POPE	MME
Siglip	384 × 384	14 × 14	728 × 1152	0.428	670.89	75.5	59.2	44.1	85.7	1179.0
TinyCLIP-39M	224 × 224	16 × 16	196 × 512	0.038	15.04	67.1	52.9	31.1	79.2	1069.5
TinyCLIP-40M	224 × 224	32 × 32	49 × 512	0.039	3.93	64.2	51.9	30.8	77.9	1022.3
TinyCLIP-61M	224 × 224	32 × 32	49 × 640	0.061	6.10	63.7	51.5	34.4	77.6	1010.2

To further reduce this cost, we explore the use of smaller vision encoders to evaluate model performance under minimized computational demands. Specifically, we compare the performance of TinyCLIP series [30] and Siglip as vision encoders, using TinyLlama-1.1B as the language decoder. The results are shown in Table 6.

For TinyCLIP-39M and TinyCLIP-40M, While these two encoders have the same feature dimensions, TinyCLIP-39M has a smaller patch size, enabling finer-grained image processing. Results show that TinyCLIP-39M outperformed across metrics. For TinyCLIP-40M and TinyCLIP-61M, Although these encoders have the same token count, TinyCLIP-61M features a larger dimensionality. However, increasing feature dimensions did not enhance performance. Instead, patch size, which affects feature sequence length, exerts a more substantial impact.

While using a smaller vision encoder reduces overall performance, it also achieves a substantial reduction in computational cost. In scenarios with stringent constraints on computational resources, such as deployment on edge/mobile devices, HiMix with a smaller vision encoder can greatly facilitate the feasibility of deploying LVLMs.

Some additional experimental results and visualizations have been provided in the [Appendix](#).

5. Discussion and conclusion

Discussion. The reduction in computational workload implies an improvement in inference speed and a decrease in computational resource consumption, which is extremely valuable in scenarios that require real-time computing analysis or need to consider device power consumption. Due to constraints in computational resources, our experiments were conducted on smaller-scale LLMs. We intend to expand our evaluations to larger models to provide a more comprehensive view of HiMix.

Conclusion. The conventional information interaction in LVLMs suffers from high computational costs, caused by vision sequences in LLM module computation. To address this issue, this paper introduces a novel mechanism for vision-language interaction, proposing a Mixture Attention module that restructures the composition and interaction of the LLM input sequence, significantly reducing the overall computational load in LVLMs. Furthermore, we develop a hierarchical injection mixture attention architecture to improve the model performance by integrating diverse vision information at specific stages within the LLM. Extensive experimental results across multiple LVLMs validate the effectiveness of our approach. Our method not only reduces computational complexity substantially but also maintains performance comparable to that of original LVLMs, showing strong potential to meet a wider range of application requirements.

References

- [1] Josh Achiam, Steven Adler, Sandhini Agarwal, Lama Ahmad, Ilge Akkaya, Florencia Leoni Aleman, Diogo Almeida, Janko Altenschmidt, Sam Altman, Shyamal Anadkat, et al. Gpt-4 technical report. *arXiv preprint arXiv:2303.08774*, 2023. 1, 2
- [2] Jean-Baptiste Alayrac, Jeff Donahue, Pauline Luc, Antoine Miech, Iain Barr, Yana Hasson, Karel Lenc, Arthur Mensch, Katherine Millican, Malcolm Reynolds, et al. Flamingo: a visual language model for few-shot learning. *Advances in neural information processing systems*, 35:23716–23736, 2022. 2
- [3] Anas Awadalla, Irena Gao, Josh Gardner, Jack Hessel, Yusuf Hanafy, Wanrong Zhu, Kalyani Marathe, Yonatan Bitton, Samir Yitzhak Gadre, Shiori Sagawa, Jenia Jitsev, Simon Kornblith, Pang Wei Koh, Gabriel Ilharco, Mitchell Wortsman, and Ludwig Schmidt. Openflamingo: An open-source framework for training large autoregressive vision-language models. *ArXiv*, abs/2308.01390, 2023. 1
- [4] Jinze Bai, Shuai Bai, Yunfei Chu, Zeyu Cui, Kai Dang, Xiaodong Deng, Yang Fan, Wenbin Ge, Yu Han, Fei Huang, et al. Qwen technical report. *arXiv preprint arXiv:2309.16609*, 2023. 2
- [5] Jinze Bai, Shuai Bai, Shusheng Yang, Shijie Wang, Sinan Tan, Peng Wang, Junyang Lin, Chang Zhou, and Jingren Zhou. Qwen-vl: A frontier large vision-language model with versatile abilities. *ArXiv*, abs/2308.12966, 2023. 2, 3
- [6] Rohan Bavishi, Erich Elsen, Curtis Hawthorne, Maxwell Nye, Augustus Odena, Arushi Somani, and Saĝnak Taşırilar. Introducing our multimodal models, 2023. 2
- [7] Mu Cai, Jianwei Yang, Jianfeng Gao, and Yong Jae Lee. Matryoshka multimodal models. *arXiv preprint arXiv:2405.17430*, 2024. 3
- [8] Lin Chen, Jinsong Li, Xiaoyi Dong, Pan Zhang, Conghui He, Jiaqi Wang, Feng Zhao, and Dahua Lin. Sharegpt4v: Improving large multi-modal models with better captions. *arXiv preprint arXiv:2311.12793*, 2023. 6
- [9] Liang Chen, Haozhe Zhao, Tianyu Liu, Shuai Bai, Junyang Lin, Chang Zhou, and Baobao Chang. An image is worth 1/2 tokens after layer 2: Plug-and-play inference acceleration for large vision-language models, 2024. 1
- [10] Liang Chen, Haozhe Zhao, Tianyu Liu, Shuai Bai, Junyang Lin, Chang Zhou, and Baobao Chang. An image is worth 1/2 tokens after layer 2: Plug-and-play inference acceleration for large vision-language models. In *European Conference on Computer Vision*, pages 19–35. Springer, 2025. 3
- [11] Zhe Chen, Jiannan Wu, Wenhai Wang, Weijie Su, Guo Chen, Sen Xing, Muyan Zhong, Qinglong Zhang, Xizhou Zhu, Lewei Lu, et al. Internvl: Scaling up vision foundation models and aligning for generic visual-linguistic tasks. In *Proceedings of the IEEE/CVF Conference on Computer Vision and Pattern Recognition*, pages 24185–24198, 2024. 2, 3
- [12] Wei-Lin Chiang, Zhuohan Li, Zi Lin, Ying Sheng, Zhanghao Wu, Hao Zhang, Lianmin Zheng, Siyuan Zhuang, Yonghao Zhuang, Joseph E Gonzalez, et al. Vicuna: An open-source chatbot impressing gpt-4 with 90%* chatgpt quality. *See https://vicuna.lmsys.org (accessed 14 April 2023)*, 2(3):6, 2023. 1
- [13] Wenliang Dai, Junnan Li, Dongxu Li, Anthony Meng Huat Tiong, Junqi Zhao, Weisheng Wang, Boyang Albert Li, Pascale Fung, and Steven C. H. Hoi. Instructblip: Towards general-purpose vision-language models with instruction tuning. *ArXiv*, abs/2305.06500, 2023. 1
- [14] Abhimanyu Dubey, Abhinav Jauhri, Abhinav Pandey, Abhishek Kadian, Ahmad Al-Dahle, Aiesha Letman, Akhil Mathur, Alan Schelten, Amy Yang, Angela Fan, et al. The llama 3 herd of models. *arXiv preprint arXiv:2407.21783*, 2024. 1, 5
- [15] Chaoyou Fu, Peixian Chen, Yunhang Shen, Yulei Qin, Mengdan Zhang, Xu Lin, Zhenyu Qiu, Wei Lin, Jinrui Yang, Xiawu Zheng, Ke Li, Xing Sun, and Rongrong Ji. Mme: A comprehensive evaluation benchmark for multimodal large language models. *ArXiv*, abs/2306.13394, 2023. 6, 7, 2
- [16] Tao Gong, Chengqi Lyu, Shilong Zhang, Yudong Wang, Miao Zheng, Qianmengke Zhao, Kuikun Liu, Wenwei Zhang, Ping Luo, and Kai Chen. Multimodal-gpt: A vision and language model for dialogue with humans. *ArXiv*, abs/2305.04790, 2023. 1
- [17] Yash Goyal, Tejas Khot, Douglas Summers-Stay, Dhruv Batra, and Devi Parikh. Making the v in vqa matter: Elevating the role of image understanding in visual question answering. In *Proceedings of the IEEE conference on computer vision and pattern recognition*, pages 6904–6913, 2017. 5, 7, 2
- [18] Drew A Hudson and Christopher D Manning. Gqa: A new dataset for real-world visual reasoning and compositional question answering. In *Proceedings of the IEEE/CVF conference on computer vision and pattern recognition*, pages 6700–6709, 2019. 5, 7, 2
- [19] Bo Li, Yuanhan Zhang, Dong Guo, Renrui Zhang, Feng Li, Hao Zhang, Kaichen Zhang, Yanwei Li, Ziwei Liu, and Chunyuan Li. Llava-onevision: Easy visual task transfer. *ArXiv*, abs/2408.03326, 2024. 2, 1
- [20] Junnan Li, Dongxu Li, Caiming Xiong, and Steven Hoi. Blip: Bootstrapping language-image pre-training for unified vision-language understanding and generation. In *International conference on machine learning*, pages 12888–12900. PMLR, 2022. 1
- [21] Junnan Li, Dongxu Li, Silvio Savarese, and Steven Hoi. Blip-2: Bootstrapping language-image pre-training with frozen image encoders and large language models. In *International conference on machine learning*, pages 19730–19742. PMLR, 2023. 1, 2
- [22] Yifan Li, Yifan Du, Kun Zhou, Jinpeng Wang, Wayne Xin Zhao, and Ji-Rong Wen. Evaluating object hallucination in large vision-language models. *arXiv preprint arXiv:2305.10355*, 2023. 6, 7, 2
- [23] Zhihang Lin, Mingbao Lin, Luxi Lin, and Rongrong Ji. Boosting multimodal large language models with visual tokens withdrawal for rapid inference. *arXiv preprint arXiv:2405.05803*, 2024. 3
- [24] Haotian Liu, Chunyuan Li, Yuheng Li, and Yong Jae Lee. Improved baselines with visual instruction tuning. 2024

- IEEE/CVF Conference on Computer Vision and Pattern Recognition (CVPR)*, pages 26286–26296, 2023. 2
- [25] Haotian Liu, Chunyuan Li, Qingyang Wu, and Yong Jae Lee. Visual instruction tuning. *Advances in neural information processing systems*, 36, 2024. 1, 2, 6
- [26] Yuzhang Shang, Mu Cai, Bingxin Xu, Yong Jae Lee, and Yan Yan. Llava-prumerge: Adaptive token reduction for efficient large multimodal models. *arXiv preprint arXiv:2403.15388*, 2024. 3
- [27] Amanpreet Singh, Vivek Natarajan, Meet Shah, Yu Jiang, Xinlei Chen, Dhruv Batra, Devi Parikh, and Marcus Rohrbach. Towards vqa models that can read. In *Proceedings of the IEEE/CVF conference on computer vision and pattern recognition*, pages 8317–8326, 2019. 6, 7, 2
- [28] Gemma Team, Thomas Mesnard, Cassidy Hardin, Robert Dadashi, Surya Bhupatiraju, Shreya Pathak, Laurent Sifre, Morgane Rivière, Mihir Sanjay Kale, Juliette Love, et al. Gemma: Open models based on gemini research and technology. *arXiv preprint arXiv:2403.08295*, 2024. 2
- [29] Hugo Touvron, Thibaut Lavril, Gautier Izacard, Xavier Martinet, Marie-Anne Lachaux, Timothée Lacroix, Baptiste Rozière, Naman Goyal, Eric Hambro, Faisal Azhar, et al. Llama: open and efficient foundation language models. *arxiv. arXiv preprint arXiv:2302.13971*, 2023. 2
- [30] Kan Wu, Houwen Peng, Zhenghong Zhou, Bin Xiao, Mengchen Liu, Lu Yuan, Hong Xuan, Michael Valenzuela, Xi Stephen Chen, Xinggang Wang, et al. Tinyclip: Clip distillation via affinity mimicking and weight inheritance. In *Proceedings of the IEEE/CVF International Conference on Computer Vision*, pages 21970–21980, 2023. 8
- [31] xiaoju ye. calfflops: a flops and params calculate tool for neural networks in pytorch framework, 2023. 3
- [32] An Yang, Baosong Yang, Binyuan Hui, Bo Zheng, Bowen Yu, Chang Zhou, Chengpeng Li, Chengyuan Li, Dayiheng Liu, Fei Huang, et al. Qwen2 technical report. *arXiv preprint arXiv:2407.10671*, 2024. 5, 1
- [33] Weihao Yu, Zhengyuan Yang, Linjie Li, Jianfeng Wang, Kevin Lin, Zicheng Liu, Xinchao Wang, and Lijuan Wang. Mm-vet: Evaluating large multimodal models for integrated capabilities. *ArXiv*, abs/2308.02490, 2023. 6, 7, 2
- [34] Xiang Yue, Yuansheng Ni, Kai Zhang, Tianyu Zheng, Ruoqi Liu, Ge Zhang, Samuel Stevens, Dongfu Jiang, Weiming Ren, Yuxuan Sun, et al. Mmmu: A massive multi-discipline multimodal understanding and reasoning benchmark for expert agi. In *Proceedings of the IEEE/CVF Conference on Computer Vision and Pattern Recognition*, pages 9556–9567, 2024. 6, 7, 2
- [35] Aohan Zeng, Xiao Liu, Zhengxiao Du, Zihan Wang, Hanyu Lai, Ming Ding, Zhuoyi Yang, Yifan Xu, Wendi Zheng, Xiao Xia, et al. Glm-130b: An open bilingual pre-trained model. *arXiv preprint arXiv:2210.02414*, 2022. 2
- [36] Xiaohua Zhai, Basil Mustafa, Alexander Kolesnikov, and Lucas Beyer. Sigmoid loss for language image pre-training. In *Proceedings of the IEEE/CVF International Conference on Computer Vision*, pages 11975–11986, 2023. 5
- [37] Peiyuan Zhang, Guangtao Zeng, Tianduo Wang, and Wei Lu. Tynllama: An open-source small language model. *arXiv preprint arXiv:2401.02385*, 2024. 2, 5, 1
- [38] Baichuan Zhou, Ying Hu, Xi Weng, Junlong Jia, Jie Luo, Xien Liu, Ji Wu, and Lei Huang. Tynllava: A framework of small-scale large multimodal models. *arXiv preprint arXiv:2402.14289*, 2024. 2, 5, 6
- [39] Deyao Zhu, Jun Chen, Xiaoqian Shen, Xiang Li, and Mohamed Elhoseiny. Minigt-4: Enhancing vision-language understanding with advanced large language models. *arXiv preprint arXiv:2304.10592*, 2023. 1, 2

HiMix: Reducing Computational Complexity in Large Vision-Language Models

Supplementary Material

In the supplementary materials, the following sections are included:

- **Implementation Details in Section A.**

This section provides a comprehensive description of the experimental setup, including detailed parameter settings. The aim is to ensure the reproducibility and clarity of the experiments.

- **Additional Experimental Results in Section B.**

This section consists of two parts: a detailed comparison of other methods and HiMix, and an in-depth breakdown of HiMix’s computational costs.

- **Qualitative Results in Section C.**

This section showcases detailed visualizations of the performance of HiMix across various tasks.

A. Implementation Details

Table 7 summarizes the detailed hyperparameters used during training under the Regular Paradigm. For the Enhanced Paradigm, the hyperparameters for the Further Pretraining and Finetuning stages are identical to those in the Finetuning stage of the Regular Paradigm. All experiments are conducted on NVIDIA A100 GPUs.

Table 7. Hyperparameter Settings for Pretrain and Finetune

Parameter	Pretrain	Finetune
Training Modules	Vision Proj	Language Decoder
Learning Rate	1e-3	2e-5
Batch Size	256	128
LR Schedule	Cosine decay	
Optimizer	AdamW	
Weight Decay	0	
Zero Stage	Zero 3	
Warmup Ratio	0.03	
Data Precision	bf16	
Attention	Flash Attention 2	

As projection layers for processing vision information are newly added to each layer of the Language Decoder and are randomly initialized, the number of training epochs is adjusted for different models to ensure sufficient training. Specifically:

- For the Qwen [32] and Llama [14] series, the pretraining stage is conducted over three epochs.
- For the TinyLlama [37], the pretraining stage is conducted over ten epochs.

- For all models, the Further Pretraining stage is conducted over one epoch, and the Finetuning stage is conducted over three epochs.

B. Additional Results

B.1. Complementary Experiment on 7B Model

HiMix employs vision projection layers to obtain richer visual features, resulting in an increase in model parameters compared to the original model. According to the Scaling Law, model performance typically improves with an increase in the number of parameters and the amount of training data. If model parameters are increased without a corresponding increase in training data, the model may not fully realize its potential. Therefore, to achieve optimal performance with HiMix, we augment the training data. The training data is sourced from LLaVA-OneVision [19], with approximately 4M data used during the pretrain stage (from LLaVA-OneVision Stage 1.5) and about 3.2M data during the finetuning stage (from LLaVA-OneVision Stage 2-SI). The visual encoder is Siglip, and the language decoder is Vicuna-7b. Both the original model and the HiMix are trained for one epoch in each of the two stages, with results presented in Table 8. Compared to the original model, HiMix achieves similar performance while reducing the computational load of the decoder to only 12%. Both Table 8 and the experimental results in the main paper demonstrate that HiMix can significantly reduce computational overhead while maintaining performance, regardless of whether applied to small-scale or large-scale MLLMs.

B.2. Comparison with Other Methods

In the Related Work section of the main paper, we introduced several approaches to Vision Token Reduction. To comprehensively evaluate our proposed method, we select one of the most competitive methods, FastV (ECCV 2024 Oral) [9], and compare it with our proposed method, HiMix. FastV introduces a dynamic image tokens pruning method to reduce the inference cost of LVLMs. In contrast, HiMix avoids the forward propagation of the entire vision sequence in the language decoder, instead leveraging a mixture attention mechanism to interact with the language at specific stages within each layer.

As shown in Table 9, we present a detailed comparison of FastV and HiMix in terms of both model performance and computational efficiency. Using Llama3-1B as the baseline model, we evaluate FastV under various parameter configurations and compare it against HiMix. While FastV achieves a reduction in computational cost compared to the

Table 8. Comprehensive comparison of performance and computational efficiency between the original model and HiMix, using SigLIP as the vision encoder. Performance metrics include VQA_{v2}, GQA, TextVQA, MM-Vet, POPE, MME, and MMMU. Computational efficiency is assessed by Language Decoder parameter count (B) and GFLOPs. Performance improvements are highlighted in **bold**, with computational cost shown in **red** as a percentage of the original model.

Language Decoder	Performances							Efficiency	
	VQA ^{v2} [17]	GQA [18]	VQA ^T [27]	MM-Vet [33]	POPE [22]	MME [15]	MMMU [34]	Params (B)	FLOPs (G)
Vicuna-7B	80.6	63.3	63.7	40.0	86.6	1439.1	36.4	7.19	10800
+HiMix	80.3	62.4	61.4	37.5	87.4	1498.9	38.3	7.47	1310(12%)

Table 9. Performance and computational efficiency comparison of Llama3-1B, FastV (under different configurations with K for filtering layer and R for filtering ratio), and HiMix. FLOPs are computed under an input configuration of V:L=728:64.

Language Decoder	VQA ^{v2} [17]	GQA [18]	VQA ^T [27]	MM-Vet [33]	POPE [22]	MMMU [34]	FLOPs (G)	FLOPs Ratio
Llama3-1B	76.8	59.6	52.7	27.8	86.7	30.6	2040	100%
+FastV (K=2 R=90%)	62.9	51.0	42.6	17.4	71.9	30.0	510	25%
+FastV (K=2 R=75%)	72.2	56.3	48.4	24.5	84.1	29.8	758	37%
+FastV (K=2 R=50%)	75.4	58.9	50.7	26.5	87.6	30.8	1180	58%
+FastV (K=3 R=90%)	60.5	49.2	38.8	17.7	69.6	30.2	595	29%
+FastV (K=3 R=75%)	70.8	55.1	45.5	24.0	82.8	30.3	829	41%
+FastV (K=3 R=50%)	75.0	58.5	49.7	27.7	87.0	30.8	1230	60%
+FastV (K=5 R=90%)	65.8	51.5	39.9	18.3	73.6	30.0	765	38%
+FastV (K=5 R=50%)	75.6	59.0	50.3	28.6	87.2	30.8	1320	65%
+HiMix	76.2	59.6	50.5	28.4	86.6	29.9	192	9%

Table 10. Component-wise Computational Costs (FLOPs) of the Language Decoder Across Different V:L Ratios. This table provides a detailed breakdown of the FLOPs consumed by attention (denoted as F_Attn) and feed-forward networks (denoted as F_FFNN) within the language decoder for different vision-to-language input length ratios.

Method	V:L 728:32		V:L 728:64		V:L 728:200		V:L 728:728		V:L 728:1000	
	F_Attn	F_FFNN	F_Attn	F_FFNN	F_Attn	F_FFNN	F_Attn	F_FFNN	F_Attn	F_FFNN
Qwen2-0.5B	117	476	124	497	156	582	311	914	410	1085
+HiMix	15	19	20	40	44	126	166	457	248	628
TinyLlama-1.1B	420	1157	442	1206	541	1413	988	2217	1258	2631
+HiMix	37	49	55	97	136	304	513	1109	747	1523
Llama-3.2-1B	331	1224	348	1276	425	1495	768	2345	973	2783
+HiMix	41	50	56	103	119	322	411	1173	590	1611
Llama-3.2-3B	1270	3213	1333	3349	1605	3924	2783	6156	3465	7306
+HiMix	148	131	204	270	442	846	1488	3078	2101	4228

baseline, its overall performance declines significantly as the computational costs decrease (i.e., as more vision tokens are pruned). Even under its best-performing configuration (Filtering layer K=5, Vision token filtering ratio R=50%), FLOPs of FastV remain at 65% of the original model.

In sharp contrast, HiMix maintains performance comparable to the baseline while reducing FLOPs to just 9% of the original model. This represents a striking improvement in computational efficiency. HiMix demonstrates clear advantages in both model performance and efficiency, highlighting its practicality and strong potential for real-world applications where both accuracy and computational efficiency are essential.

B.3. Detailed Computational Analysis

To provide a more in-depth analysis of the efficiency results presented in the main paper, this subsection examines the computational cost breakdown within the language decoder under different input configurations. Specifically, Table 10 presents the FLOPs (in GFLOPs) consumed by the two major components of the language decoder—attention and feed-forward networks (FFN). The V:L ratio represents the lengths of the vision and language sequences in the input prompt. Computational costs are reported for both the baseline models and the proposed HiMix.

As described in Equation 7 of the main paper, HiMix avoids the quadratic complexity of Vanilla-LVLM in the attention mechanism. For the FFN, the vision sequence is excluded entirely from computation, which significantly reduces the overall computational cost.

The results highlight HiMix’s ability to optimize the computational cost of the language decoder while preserving performance metrics, positioning it as a practical solution for deploying LVLMs in resource-constrained scenarios with a strong balance between accuracy and efficiency.

The tool used for testing FLOPs is [31].

C. Qualitative Results

This section provides qualitative results to offer a more intuitive understanding and comparison between the baseline model (e.g., Llama3-1B) and HiMix. Specifically, we showcase multiple tasks, including choice questions (Figure 6), yes/no questions (Figure 7), simple image captions and detailed image captions (Figures 8, 9, and 10), object recognition (Figure 11) and text OCR (Figure 12). We observe the following results:

- HiMix achieves performance comparable to the baseline. Across various multimodal tasks, HiMix accurately understands and responds to the requirements, demonstrating strong alignment with task-specific objectives.
- When the task requires detailed image descriptions, both the baseline model and HiMix occasionally generate similar hallucinated descriptions (highlighted in red in the images). We attribute this behavior to the inherent limitations of the selected baseline model. Nevertheless, these results confirm that HiMix does not compromise the baseline model’s ability to process and interpret vision information, maintaining performance parity with the baseline model.
- As discussed in the main paper, HiMix exhibits a slight decline in OCR capabilities. We present examples of failure cases to illustrate this limitation. However, under the Enhanced Paradigm, this drawback is mitigated, demonstrating that training data augmentation effectively improves performance.

Choice Questions

	<table border="1"> <thead> <tr> <th colspan="2">McDougal Printing, Inc. Year Ended December 31, 2015</th> </tr> </thead> <tbody> <tr> <td>Sales</td> <td>\$40,000,000</td> </tr> <tr> <td>Gross profit margin</td> <td>80%</td> </tr> <tr> <td>Operating profit margin</td> <td>35%</td> </tr> <tr> <td>Net profit margin</td> <td>8%</td> </tr> <tr> <td>Return on total assets</td> <td>16%</td> </tr> <tr> <td>Return on common equity</td> <td>20%</td> </tr> <tr> <td>Total asset turnover</td> <td>2</td> </tr> <tr> <td>Average collection period</td> <td>62.2 days</td> </tr> </tbody> </table>	McDougal Printing, Inc. Year Ended December 31, 2015		Sales	\$40,000,000	Gross profit margin	80%	Operating profit margin	35%	Net profit margin	8%	Return on total assets	16%	Return on common equity	20%	Total asset turnover	2	Average collection period	62.2 days	
McDougal Printing, Inc. Year Ended December 31, 2015																				
Sales	\$40,000,000																			
Gross profit margin	80%																			
Operating profit margin	35%																			
Net profit margin	8%																			
Return on total assets	16%																			
Return on common equity	20%																			
Total asset turnover	2																			
Average collection period	62.2 days																			
<p>Question: What is the title of this design?</p> <p>(A) Zenith Guardian Ear & Radio Nurse (B) Innovative Hearing Aid Technology (C) Ear and Radio Communication Advancements (D) The Future of Guardian Technology</p> <p>Llama3-1B: A HiMix: A</p>	<p>Question: McDougal, Inc., had sales totaling \$40,000,000 in fiscal year 2015. Some ratios for the company are listed below. Use this information to calculate values for the operating profits.</p> <p>(A) \$14,000,000 (B) \$8,000,000 (C) \$32,000,000 (D) \$18,000,000</p> <p>Llama3-1B: A HiMix: A</p>	<p>Question: Identify the biome shown in image</p> <p>(A) taiga (B) tundra (C) rain forest (D) desert</p> <p>Llama3-1B: B HiMix: B</p>																		

Figure 6. Qualitative results of choice questions.

Yes-or-No Questions

		
<p>Question: Is there a person in the image?</p> <p>Llama3-1B: Yes HiMix: Yes</p> <p>Question: Is there a dining table in the image?</p> <p>Llama3-1B: No HiMix: No</p>	<p>Question: Is there a broccoli in the image?</p> <p>Llama3-1B: Yes HiMix: Yes</p> <p>Question: Is there a dining table in the image?</p> <p>Llama3-1B: Yes HiMix: No</p>	<p>Question: Is there a dog in the image?</p> <p>Llama3-1B: No HiMix: No</p> <p>Question: Is there a tennis racket in the image?</p> <p>Llama3-1B: No HiMix: No</p>

Figure 7. Qualitative results of yes/no questions. Correct answers and Wrong answers are highlighted in color respectively.

Image Caption



Generate a simple caption for this image.

Llama3-1B: A group of **children playing** a video game in a living room.

HiMix: A group of four **people are playing** a video game in a living room.

Generate a detailed description of this image.

Llama3-1B: The image depicts a group of four young boys **playing a video game** together in a living room. They are standing in front of a window, which is partially open, **allowing natural light to enter the room**. The boys are **holding game controllers**, actively engaged in the game. In the room, there are two chairs. A couch can be seen in the background, occupying the right side of the room.

HiMix: The image shows a group of four people, including two boys and two girls, standing in a living room and **playing a video game** together. They are all holding **Wii controllers** and appear to be enjoying the game. The living room is furnished with a couch and a couple of chairs, providing a comfortable space for the group to play and socialize.



Generate a simple caption for this image.

Llama3-1B: A man **holding a fish** in front of a river.

HiMix: A man wearing a hat and a suit is **holding a fish** he caught.

Generate a detailed description of this image.

Llama3-1B: The image features a man **wearing a hat and a suit**, standing by a river with a large **fish in his hand**. He is holding the fish **with pride**, showcasing his catch. The man appears to be a fisherman, possibly posing for a picture with the fish he has just caught.

HiMix: The image features a man **wearing a hat and a suit**, **holding a large fish** he has caught in his hands. He is posing for a picture while **proudly** displaying his catch. The man is standing near a body of water, which could be a river or a lake, as he is holding a fish that he caught in that location.

Figure 8. Qualitative comparison of image captions. **Correct descriptions** and **hallucinated** are highlighted in color respectively.

Image Caption



Generate a simple caption for this image.

Llama3-1B: A **soccer player** in a red and white uniform is **jumping** in the air.

HiMix: A **soccer player** wearing red and white **jumps** in mid air.

Generate a detailed description of this image.

Llama3-1B: The image captures a lively soccer game in progress, with a **player in red and white uniform** leaping into the air to kick the ball. The player is in the middle of the field, surrounded by **several other players** and spectators. A sports ball can be seen in the middle of the field.

HiMix: The image features a soccer field with a **man wearing a red and white striped uniform**, standing in the air and jumping to catch a soccer ball. He is in the process of making a powerful leap, showcasing his athleticism. In the background, there are **several other people** scattered around the field, possibly watching the game or waiting for their turn to play.



Generate a simple caption for this image.

Llama3-1B: A **cat** is sitting in a **toilet bowl** and looking at the camera.

HiMix: A **cat** is sitting in a **toilet bowl** and looking up.

Generate a detailed description of this image.

Llama3-1B: The image features a **brown and white cat sitting inside a toilet bowl**. The cat appears to be enjoying its time in the toilet, as it is comfortably curled up and resting. **The toilet bowl is filled with water**, creating a unique and amusing scene for the cat.

HiMix: The image features a **large, fluffy orange and white cat** sitting inside a toilet bowl. The cat appears to be relaxed and comfortable, with its paws up and resting on the toilet seat. **The toilet bowl is filled with water**, creating a unique scene of the cat enjoying its time in the bathroom.

Figure 9. Qualitative comparison of image captions. **Correct descriptions** and **hallucinated** are highlighted in color respectively.

Image Caption



Generate a simple caption for this image.

Llama3-1B: A dog is holding a hot dog in its mouth.

HiMix: A dog is holding a hot dog in its mouth and wearing a collar.



Generate a simple caption for this image.

Llama3-1B: A man riding a surfboard in the ocean.

HiMix: A surfer wearing a red shirt riding a wave on a surfboard.

Generate a detailed description of this image.

Llama3-1B: The image features a black and white dog sitting on a green chair, holding a hot dog in its mouth. The dog appears to be enjoying the hot dog, as it is smiling and chewing on it. The chair is positioned in the center of the scene, with the dog occupying the majority of the frame.

HiMix: The image features a black and white dog wearing a red collar, lying on a green bean bag chair and enjoying a hot dog. The dog appears to be chewing on the hot dog, which is placed in its mouth. The scene is set in a cozy environment, with the dog comfortably resting on the bean bag chair.

Generate a detailed description of this image.

Llama3-1B: The image captures a thrilling moment of a man riding a wave on a surfboard. He is skillfully maneuvering through the water, showcasing his expertise in surfing. In addition to the main surfer, there are two other people visible in the scene. One person is located towards the left side of the image, and the other person is positioned slightly to the right of the main surfer. Both of them appear to be enjoying the ocean waves as well.

HiMix: The image features a man riding a surfboard on a wave in the ocean. He is skillfully maneuvering his surfboard, making a turn as he rides the wave. The surfer is wearing a red shirt, which stands out against the blue ocean water. There are several other smaller waves in the scene, some of which are also being ridden by surfers. The surfers are spread out across the ocean, with some closer to the shore and others further out in the water.

Figure 10. Qualitative comparison of image captions. Correct descriptions and hallucinated are highlighted in color respectively.

Object Recognition		
		
<p>Question: What type of animal is shown in the image?</p> <p>Llama3-1B: The image shows a dog.</p> <p>HiMix: The image shows a dog.</p>	<p>Question: What kind of animal is visible in the image?</p> <p>Llama3-1B: A donkey is visible in the image.</p> <p>HiMix: A donkey is visible in the image.</p>	<p>Question: Can you describe the clothes worn by the people in the picture?</p> <p>Llama3-1B: One woman is wearing a blue shirt, another is wearing a white shirt, and the third woman is wearing a blue sweater.</p> <p>HiMix: One the woman is wearing a white shirt, and the two other people are dressed in blue clothing.</p>
<p>Question: What are they playing?</p> <p>Llama3-1B: The woman and a brown dog are playing Frisbee.</p> <p>HiMix: The woman and dog are playing Frisbee together in a grassy field.</p>	<p>Question: Can you identify the type of object being offered to the animal?</p> <p>Llama3-1B: The object being offered to the animal is a carrot.</p> <p>HiMix: Yes, the object being offered to the animal is a carrot.</p>	<p>Question: Which person in the picture is carrying a bag? What colour is it?</p> <p>Llama3-1B: In the picture, the woman in the blue shirt is carrying a black bag.</p> <p>HiMix: The person in the picture carrying a black bag is a woman wearing a white jacket.</p>

Figure 11. Qualitative results of object recognition tasks. Correctly identified objects and errors are highlighted in color respectively.

TextOCR Questions		
		
<p>Question: Is the word in the logo "kress"?</p> <p>Llama3-1B: Yes</p> <p>HiMix: Yes</p> <p>HiMix-Enhanced: Yes</p>	<p>Question: Is the text in the picture "hollywood"?</p> <p>Llama3-1B: Yes</p> <p>HiMix: Yes</p> <p>HiMix-Enhanced: Yes</p>	<p>Question: Is the word in the logo "shop rite"?</p> <p>Llama3-1B: Yes</p> <p>HiMix: Yes</p> <p>HiMix-Enhanced: Yes</p>
<p>Question: Is the word in the logo "dress"?</p> <p>Llama3-1B: No</p> <p>HiMix: No</p> <p>HiMix-Enhanced: No</p>	<p>Question: Is the text in the picture "holly word"?</p> <p>Llama3-1B: No</p> <p>HiMix: Yes</p> <p>HiMix-Enhanced: No</p>	<p>Question: Is the word in the logo "stop rite"?</p> <p>Llama3-1B: No</p> <p>HiMix: Yes</p> <p>HiMix-Enhanced: No</p>

Figure 12. Qualitative results of text OCR tasks. Correctly recognized text and errors are highlighted for comparison.